The non-Gaussian nature of fracture and the survival of fat-tail exponents

Ken Tore Tallakstad, Renaud Toussaint, Stéphane Santucci, Knut Jørgen Måløy

▶ **To cite this version:**

HAL Id: hal-00816217

https://hal.archives-ouvertes.fr/hal-00816217

Submitted on 20 Apr 2013

The non-Gaussian nature of fracture and the survival of fat-tail exponents

Ken Tore Tallakstad,[1] Renaud Toussaint,[2, 3] Stephane Santucci,[4, 3] and Knut Jørgen Måløy[1, 3]

[1]*Department of Physics, University of Oslo, PB 1048 Blindern, NO-0316 Oslo, Norway*
[2]*Institut de Physique du Globe de Strasbourg, UMR 7516 CNRS,*
Université de Strasbourg, 5 rue René Descartes, F-67084 Strasbourg Cedex, France
[3]*Centre for Advanced Study at The Norwegian Academy of Science and Letters, Drammensveien 78, 0271 N-Oslo, Norway*
[4]*Laboratoire de Physique, Ecole Normale Supérieure de Lyon, CNRS UMR 5672, 46 Allée d'Italie, 69364 Lyon cedex 07, France*
(ΩDated: January 24, 2013)

We study the fluctuations of the global velocity $V_l(t)$, computed at various length scales l, during the intermittent Mode-I propagation of a crack front. The statistics converge to a non-Gaussian distribution, with an asymmetric shape and a fat tail. This breakdown of the Central Limit Theorem (*CLT*), is due to the diverging variance of the underlying local crack front velocity distribution, displaying a power law tail [1, 2]. Indeed, by the application of a generalized CLT, the full shape of our experimental velocity distribution at large scale is shown to follow the *stable Levy* distribution, which preserves the power law tail exponent under upscaling. This study aims to demonstrate in general for Crackling Noise systems, how one can infer the complete scale dependence of the activity- and extreme event distributions, by measuring only at a global scale.

PACS numbers: 62.20.mt, 46.50.+a, 68.35.Ct

The failure of heterogeneous materials is a complex process taking place on a very broad range of scales; from the separation of atomic bonds, to the nucleation and growth of micro and macro voids, even up to earthquakes and fault dynamics [3, 4]. The competition between pinning forces, at local asperities of high toughness, and long range elastic forces due to loading, results both in a rough fracture morphology, with self-affine scaling properties [5–7], and a complex intermittent dynamics. The velocity fluctuations are very large, containing sudden avalanches that span a wide range of sizes and durations [1, 2, 8]. Such a complex spatiotemporal dynamics, generically called *Crackling Noise* [9], arises also in a wide variety of other physical systems, for instance, magnetic domain wall motion in disordered ferromagnets [10], vortex lines in type-II superconductors [11], and dislocation lines in defective crystalline solids [12]. However, in most systems, experimentally, one usually cannot access the local information, as for instance a front position as function of space and time, $h(x, y, t)$. Thus, the crackling dynamics can only be characterized at a global scale, via the measurement of a global, i.e. spatially averaged, quantity. This is particularly the case for the fracture of disordered materials, where the damaging processes are usually monitored indirectly via the recording of acoustic emissions [13–15], since the materials considered are usually opaque and the crack fronts have a complex 3d structure, therefore preventing a direct observation.

We overcome such difficulty, by using a transparent model where the crack is constrained to propagate along a weak heterogeneous interface [2]. Thus, using a high resolution fast camera, we extract, in all details, the *local spatio-temporal* crack front dynamics. Specifically, we have shown previously that the dynamics is governed by avalanches with very large size and velocity fluctua-

tions, following a fat-tail distribution with a power law exponent $1 + \alpha = 2.6 \pm 0.15$, and thus has a diverging variance [1, 2]. This theoretically implies the breakdown of the usual CLT [16]. In the present Letter, we exploit our detailed local information, and go further on the investigation of such complex dynamics at larger scales.

We focus now on the global crack growth, which displays an intermittent behavior, as a consequence of the local burst motion of the front. We study in particular the fluctuations of the global velocity $V_l(t)$, spatially averaged at different length scales, and show that they do not converge to the usual Gaussian statistics. Interestingly, recent theoretical and experimental results [17–19], have underlined the importance of long range spatial correlations in the statistics of a global variable, showing that such fluctuations can follow a General Gumbel distribution – asymmetric with an exponential tail– when the measuring window is comparable to the correlation length; while above such a characteristic length scale, a clear convergence to the Gaussian statistics is observed.

In contrast, as observed in our experiments, the deviation from the Gaussian law, does not arise from finite size effects, but is due to the diverging second moment of underlying local crack front velocity *Probability Distribution Function* (PDF). As a consequence, the PDF of the sum, or average, of such local random variables does not converge to a Gaussian, but rather to a *stable Levy distribution* [16, 20]. Indeed, by using a generalization of the CLT, we can predict the full nature of the global velocity fluctuations, characterized by the fat tail scaling exponent α and an asymmetry parameter β. The main implication of this generalized CLT, is the preservation of local information also at large scale, i.e α survives averaging and can be measured, provided good enough statistics. Furthermore this can be exploited to predict the

scaling of extremes, and of the individual summands in the global variable. This is, to the best of our knowledge, the first time such Levy distributions and its formalism are reported and used in the case of fracture.

We observe directly, with a high resolution fast camera, a crack front propagating slowly $(0.1 - 100 \, \mu m/s)$ along a weak heterogeneous interface of a Plexiglas block. It is made of two weakly sintered sandblasted plates of dimension of $(27, 14, 1) \, \mathrm{cm}$ and $(30, 12, 0.4) \, \mathrm{cm}$. The roughening procedure generates heterogeneities in the range of $\sim 15 - 50 \, \mu m$ [21]. The crack front propagation is imaged at a very high spatial– (up to 3000 pixels, with a pixel size of $a \approx 2.5 \, \mu m$) and temporal resolution (up to 40000 images recorded at a rate from $1 \, fps$ up to $1000 \, fps$), relative to its velocity fluctuations. The imaged area, covered by the crack front, corresponds to roughly $(6 \times 0.5) \, \mathrm{mm}$ transverse to, and along the direction of propagation respectively. The quasi mode-I crack growth is obtained by imposing a normal displacement to the bottom plate while the upper plate is fixed to an aluminum frame[2]. Independently of the loading conditions [2], the time of observation is small enough, so that the average velocity of crack propagation in space and time is constant during an experiment.
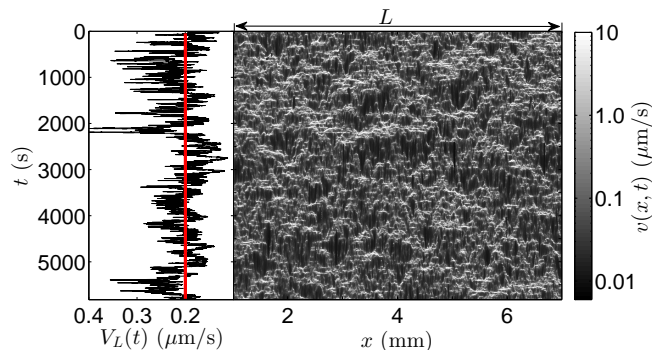

FIG. 1. Right: The spatio-temporal velocity field $v(x,t)$ during a fracture experiment. Left: The corresponding spatially averaged signal $V_L(t) = \langle v(x,t) \rangle_l$, over the full system size L. The solid red line indicates the full space-time average velocity $\langle V_L \rangle_T = \bar{v}$.

The local velocity along the crack front $h(x,t)$ is computed from the waiting time at a given position $w(x,y)$ [1, 2], i.e the discrete number of time units the front has spent at a given pixel. The local velocity of the front is then obtained for each front at each time step as: $v(x,t) = a/w[x, h(x,t)]\delta t$, where a is the pixel size and δt is the time resolution. This constitutes a local velocity *space-time* map, where the global velocity, $V_l(t)$, spatially averaged over line segments of length l (pixels) in the x-direction, can be measured at any scale l: $V_l(t) = \langle v(x,t) \rangle_l \equiv \frac{1}{l} \sum_{i=1}^{l} v(x_i, t)$, with temporal mean $\langle V_l \rangle_T = \frac{1}{T} \sum_{j=1}^{T} V_l(t_j)$, and estimated standard devia-

tion $\sigma^2 \equiv \left\langle (V_l - \langle V_l \rangle_T)^2 \right\rangle_T$, where T is the total number of time steps of the signal. To check that our results are independent of the specific way the global velocity is obtained, we compare when suitable (Figs. 2 and 3) to those obtained when the global velocity is instead computed directly, through the time derivative of the spatially averaged crack front position at scale l, $U_l(t) = d\langle h(x,t) \rangle_l/dt$. This is typically what is done in low resolution Crackling Noise experiments.

The local velocity fluctuations, in space and time, along the crack front, for $v > \bar{v}$, follow a power-law distribution, $P(v/\bar{v}) \propto (v/\bar{v})^{-(\alpha+1)}$ with $\alpha = 1.6 \pm 0.15$, independently of the loading conditions and average crack front velocity [2]. Since the mean, $\bar{v} \equiv \int_0^\infty v P(v) dv$, is well defined for $\alpha > 1$ we have: $\bar{v} = \langle V_l \rangle_T = \bar{V}_l \equiv \int_0^\infty V_l \Psi(V_l) dV_l$ for sufficiently large T, where $\Psi(V_l)$ is the PDF of V_l. Local fluctuations occur over a very broad interval, as observed on a typical space-time map of the velocity field, $v(x,t)$, shown in Fig. 1, and thus lead to a complex intermittent dynamics of the global crack growth $V_l(t)$.

The variance of a sum of independent and identically distributed random variables, equals the sum of their individual variances [16, 20], i.e $\langle (\sum_{i=1}^{l} v_i - \langle \sum_{i=1}^{l} v_i \rangle_T)^2 \rangle_T \sim l \langle \langle (v - \bar{v})^2 \rangle_l \rangle_T$, in the large T limit. Under such assumptions and by multiplying with $1/l^2$, we obtain the relationship between the global velocity V_l at scale l and the local velocity v:

$$\sigma^2 = \left\langle \left(V_l - \bar{V}_l \right)^2 \right\rangle_T \sim \frac{1}{l} \left\langle \left\langle (v - \bar{v})^2 \right\rangle_l \right\rangle_T . \quad (1)$$

For large T, the variance estimators of v can be replaced with an integral over the underlying PDF [23],

$$\left(\frac{\sigma}{\bar{v}} \right)^2 \sim \frac{1}{l} \int_0^{z^*} (z-1)^2 G(z) z^{-(1+\alpha)} dz , \quad (2)$$

where $z = v/\bar{v}$ and $G(z) = P(z) z^{1+\alpha}$ is the lower cutoff function of $P(z)$, ensuring the convergence in the lower limit (because $G(z)$ is finite for $z \ll 1$). In the upper limit $(G(z) \sim 1$ for $z \gg 1)$, this integral will diverge if $z^* \to \infty$ for $\alpha < 2$. However, since σ is only estimated over a scale l and sampled over a finite number of realizations T, z^* must be finite, and given by the largest velocities that are sampled from $P(z)$ to generate the global velocity V_l. Thus, as argued in [23], $z^* \bar{v}$ can be represented by the average maximum velocity at scale l, i.e $\langle v_{max}^l(t) \rangle_T \equiv \langle \max\{v(x_i, t); i = 1, ..., l\} \rangle_T$. From extreme value theory, the PDF of v_{max}^l will converge to the so-called *Fréchet* distribution, with mean [16, 20, 23]:

$$\langle v_{max}^l \rangle_T \sim l^\gamma , \text{ where } \gamma = 1/\alpha . \quad (3)$$

We use $z^* = \langle v_{max}^l \rangle_T / \bar{v}$ as an upper limit in Eq. (2) giving,

$$(\sigma/\bar{v}) \sim l^{-\xi} \text{ with } \xi = 1 - \frac{1}{\alpha} . \quad (4)$$

Note that for $\alpha < 2$, Eq. (4) predicts non-Gaussian statistics. For uncorrelated data, such a scaling provides an indirect way of measuring the power law exponent in the fat tail of the local variables distribution. Usually in experiments, high resolution data are unavailable. This measure should thus prove particularly useful in general.
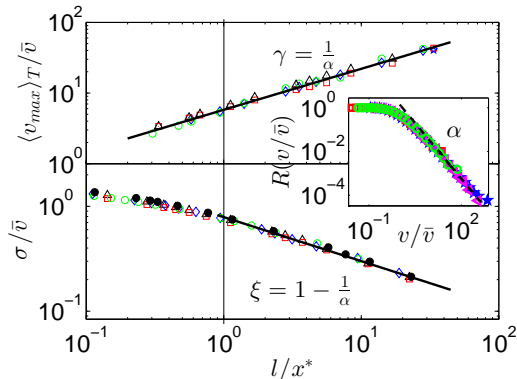

FIG. 2. Average maximum velocity (upper panel) $\langle v^l_{max}\rangle_T/\bar{v}$ and standard deviation (lower panel) $\sigma/\bar{v}$ of $V_l(t)$, as function of the measuring window rescaled by the correlation length, l/x^*. The upper solid line corresponds to the slope $\gamma = 1/1.7 \approx 0.58$. The lower solid line is a fit of Eq. (4) for $l/x^* > 3$, giving $\xi = 0.42 \pm 0.03$ and thus $\alpha = 1.7 \pm 0.1$. Circular black markers show, for one experiment, $\sigma(l)$, obtained from $U_l(t)$ (smoothed over 15 time steps) as defined in the text. The inset shows the cumulative PDF of the local velocity $R(v/\bar{v})$. The dashed line is a fit to the asymptotic tail, using $\alpha = 1.7$, to obtain λ^+ as defined in the text.

Figure 2 shows the scaling behavior of both $\langle v^l_{max}\rangle_T$ and σ, normalized by $\bar{v}$ for different experiments [2], as function of l, rescaled by the correlation length x^*. Indeed, due to the interplay between sample disorder and elastic interactions, the local velocities are correlated along the crack front, up to a characteristic scale $x^* \sim 150\,\mu$m [2]. Our data appear in excellent agreement with the expected scaling behavior, providing the exponent and $\xi = 0.42 \pm 0.02$ leading to $\gamma = 0.58 \pm 0.03$ and $\alpha = 1.7 \pm 0.1$, consistent with the value previously reported [1, 2]. Interestingly, we observe a different regime with a deviation to the expected scaling behavior for $\sigma < l/x^*$, whereas $\langle v_{max}\rangle_t$ maintains the scaling prediction even at scales below l/x^*. Hence, measuring the spatial dependence of σ or $\langle v^l_{max}\rangle_T$, at a few large scales, allows to determine the tail shape of the underlying local distribution. This is also confirmed when $\sigma(l)$ is obtained from $U_l(t)$, as shown in black circular markers in the lower panel of Fig. 2.

To predict the full shape of the global velocity PDF, measured at various scales l, consider now the normalized global velocity $V' = (V_l(t) - \langle V_l(t)\rangle_T)/b_l$, where b_l [cf. Eq. (7)] is a normalization constant. We show in the upper panel of Fig. 3, the PDF's $\Psi(V')$ for three ex-
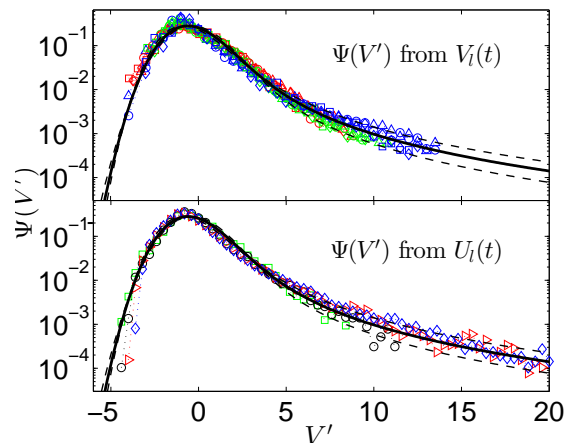

FIG. 3. (Color online) PDF $\Psi(V')$ of the global velocity $V_l(t)$ (upper panel) for three different experiments (red, green, and blue), at four different averaging scales $l/x^* \in \{40, 20, 13, 10\}$, in semi-log representation. For one of these experiments (blue), we obtain $\Psi(V')$ from $U_l(t)$, smoothed over 15 time steps, at the same averaging scales (lower panel). The solid lines show the PDF $\Psi(V'; 1.7, 1)$, obtained from Eq. (5), whereas the dashed lines correspond to $\Psi(V'; 1.7 \pm 0.1, 1)$, displaying the effect of the variations in α.

periments, at different space-time average velocity [2]: $\langle V_l\rangle_t = \bar{v} = 0.15\,\mu$m/s, $\bar{v} = 1.36\,\mu$m/s, and $\bar{v} = 141\,\mu$m/s. The global velocity V_l has been obtained over four different length scales l, at least one order of magnitude above the correlation length x^*, so that $l/x^* \approx \{40, 20, 13, 10\}$. We observe a clear data collapse of our experimental PDF's, showing a non-Gaussian behavior of the temporal fluctuations of the global velocity $V_l(t)$, with an asymmetric shape and an asymptotic fat tail for large positive values. It is important to underline that this behavior is independent of the loading conditions or average propagation velocity of the crack front. Some dispersion in the tail between the experiments is observed, however within the limits of uncertainty in α, and can be traced back to small variations in the tail for the experimental $P(v/\bar{v})$ PDF's. The lower panel in Fig. 3 shows $\Psi(V')$, where V' is now obtained through $U_l(t)$, also including more points in the tail due to slightly higher statistical significance in those data. It is evident that the two ways of obtaining the global velocity produces highly consistent results.

The fat tail decay, observed for the local velocity distribution with $\alpha + 1 = 2.7 < 3$, produces the divergence of the integral in Eq. (2), and thus leads to the breakdown of the usual CLT. However, we can explain these results by invoking a generalization of the CLT, in particular that the fat tail, seen in Fig. 3, of the experimental data should decay with a power law exponent $1 + \alpha$. It states that an average variable, V, of a number of independent random variables, v, with an asymptotic power

law tail distribution $1/|v|^{\alpha+1}$, where $\alpha < 2$ (and therefore having infinite variance) will tend to a so-called *alpha stable Levy distribution* [22], $\Psi(V; \alpha, \beta, c, \delta)$, as the number of individual variables v, used to obtain the average V, grow [16, 20]. Generally not analytically expressible, Ψ contains four parameters and is defined through the inverse Fourier transform of its characteristic function Φ,

$$\Psi(V; \alpha, \beta, c, \delta) = \frac{1}{2\pi} \int_{-\infty}^{\infty} \Phi(k) \exp(-iVk)\, dk \ , \quad (5)$$

$$\Phi(k) = \exp\left[ik\delta - |ck|^{\alpha}\left(1 + i\beta\frac{k}{|k|}\tan(\frac{\pi}{2}\alpha)\right)\right] \ , \quad (6)$$

for $\alpha \neq 1$. Here, V is the random variable (in our case the global velocity), α is the index of the distribution giving the exponent of the asymptotic power law tail ($\alpha + 1$), $\beta \in [-1, 1]$ is the so-called skewness parameter and a measure of asymmetry. Note in this context that the usual skewness, given by the third moment of the distribution [20], is not well defined for $\alpha < 2$ due to the divergence of the 2nd and higher order moments. The shift parameter δ gives the peak position for a symmetric distribution, whereas c is a scale factor characterizing its width. For $\alpha > 1$, it is possible to reduce the number of varying parameters in Ψ by the following normalization of V [20]:

$$V' = \frac{V_l - \langle V_l \rangle_T}{b_l} \ , \ \text{with } b_l = \left(\frac{\pi(\lambda^+ + \lambda^-)}{2\Gamma(\alpha)\sin(\alpha\pi/2)}\right)^{\frac{1}{\alpha}} l^{1/\alpha - 1} \ . \quad (7)$$

Here, b_l is proportional to the standard deviation, and with this normalization V' will be centered around zero, leading to $\delta = 0$, and $c = 1$. In Eq. (7), Γ is the Gamma function, whereas the constants λ^+ and λ^- characterize the asymptotic behavior on the positive and negative axis respectively, of the cumulative distribution function of v: $R(v \to \infty) = \lambda^+ v^{-\alpha}$, and $1 - R(v \to -\infty) = \lambda^-|v|^{-\alpha}$. The skewness parameter is given as, $\beta = \frac{\lambda^+ - \lambda^-}{\lambda^+ + \lambda^-}$, which has its extreme value of 1 in the case of non-negative summands v [20], as is the case here, leading to $\lambda^- = 0$ and thus, $\beta = 1$. Finally, from the cumulative PDF $R(v/\bar{v})$, shown by the dashed line in the inset in Fig. 2, we obtain $\lambda^+ \approx 1.4$. Thus, our experimental data should converge to the distribution $\Psi(V'; 1.7, 1, 1, 0) \equiv \Psi(V'; 1.7, 1)$, shown as a solid line in Fig. 3. The comparison is highly satisfactory.

Finally, we examine the rate of convergence to such a stable law, when the measuring length scale increases from the micron to the millimeter scale, below and above the correlation length respectively. This evolution is shown in Fig. 4, represented in log-log form, for the scales $l/x^* \approx \{3, 1, 0.5, 0.2, 0.05\}$, and shifted systematically for visual clarity. The solid lines show the corresponding Levy distribution $\Psi(V'; 1.7, 1)$. The convergence to the Levy law is clear, as soon as the measuring window is
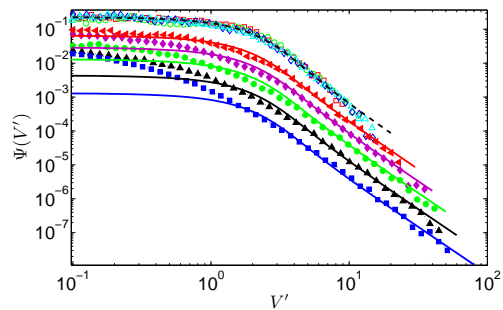

FIG. 4. (Color online) PDFs $\Psi(V')$ for one experiment in log-log representation, at the scales $l/x^* \approx \{40, 20, 13, 10\}$ (upper collapsed curves, empty markers), and in filled markers from top to bottom, at $l/x^* \approx \{3, 1, 0.5, 0.2, 0.05\}$ respectively. The latter distributions with the theoretical curves, $\Psi(V'; 1.7, 1)$ shown as solid lines, have been shifted for visual clarity.

larger than the correlation length x^*. However more strikingly, the fat tail of the velocity distribution survives clearly the upscaling. This shows very explicitly, the validity of the generalized CLT for the fracture velocity statistics.

We have analyzed the intermittent propagation of a crack front along a heterogeneous plane in a Plexiglas block, focusing on the temporal fluctuations of the global velocity, i.e. spatially averaged at various length scales. We have shown how the fat tail of the local crack front velocity leads to the breakdown of the Central Limit Theorem, with anomalous scaling behaviors of the average maximum velocity $\langle v_{max}^l \rangle_T$ and variance σ of $V_l(t)$, and thus non-Gaussian fluctuations also at the large scale. Moreover, we have demonstrated how the generalized version of the CLT must be applied, in order to predict the full global distribution of crack front velocities.

[1] K. J. Måløy, S. Santucci, J. Schmittbuhl, and R. Toussaint, Phys. Rev. Lett. **96**, 045501 (2006).
[2] K. T. Tallakstad, R. Toussaint, S. Santucci, J. Schmittbuhl, and K. J. Måløy, Phys. Rev. E **83**, 046108 (2011).
[3] M. J. Alava, P. K. V. V. Nukala, and S. Zapperi, Adv. Phys. **55**, 349 (2006).
[4] D. Bonamy and E. Bouchaud, J. Phys. Rep. **498**, 1 (2011).
[5] L. Ponson, D. Bonamy, and E. Bouchaud, Phys. Rev. Lett. **96**, 035506 (2006).
[6] S. Santucci, K. J. Måløy, A. Delaplace, J. Mathiesen, A. Hansen, J. O. Haavig Bakke, J. Schmittbuhl, L. Vanel,

and P. Ray, Phys. Rev. E **75**, 016104 (2007).

[7] J. Schmittbuhl, and K. J. Måløy, Phys. Rev. Lett. **78**, 3888 (1997).

[8] K. J. Måløy and J. Schmittbuhl, Phys. Rev. Lett. **87**, 105502 (2001).

[9] J. Sethna, K. Dahmen, and C. Myers, Nature (London) **410**, 242 (2001).

[10] D. Spasojevi, S. Bukvić, S. Milošević, and H. E. Stanley, Phys. Rev. E **54**, 2531 (1996).

[11] G. Blatter, M. V. Feigel'man, V. B. Geshkenbein, A. I. Larkin, and V. M. Vinokur, Rev. Mod. Phys. **66**, 1125 (1994).

[12] F. F. Csikor, C. Motz, D. Weygand, M. Zaiser, and S. Zapperi, Science **318**, 251 (2007).

[13] A. Garcimartín, A. Guarino, L. Bellon, and S. Ciliberto, Phys. Rev. Lett. **79**, 3202 (1997).

[14] J. Davidsen, S. Stanchits, and G. Dresen, Phys. Rev. Lett. **98**, 125502 (2007).

[15] J. Koivisto, J. Rosti, and M. J. Alava, Phys. Rev. Lett. **99**, 145504 (2007).

[16] D. Sornette, *Critical Phenomena in Natural Sciences* (Springer-Verlag, Berlin Heidelberg, Germany, 2000).

[17] E. Bertin, Phys. Rev. Lett. **95**, 170601 (2005).

[18] S. Joubaud, A. Petrosyan, S. Ciliberto, and N. B. Garnier, Phys. Rev. Lett. **100**, 180601 (2008).

[19] R. Planet, S. Santucci, and J. Ortín, Phys. Rev. Lett. **102**, 094502 (2009).

[20] V. V. Uchaikin and V. M. Zolotarev, *Chance and Stability - Stable Distributions and their Applications* (VSP BV, The Netherlands, 1999).

[21] S. Santucci, M. Grob, A. Hansen, R. Toussaint, J. Schmittbuhl, and K. J. Måløy, Euro. Phys. Lett. **92**, 44001 (2010).

[22] Note1, this family of distributions are in some communities referred to simply as *Stable Distributions*. In such a case, the term *stable Levy*, is reserved for the special case of $\alpha = 1/2$, [20].

[23] Note2, see Supplementary Information for details on Eqs. (1)–(4)

[24] M. Veillette (2008), URL `http://math.bu.edu/people/mveillet/html/alphastablepub.html`.